Desalination and Water Treatment
www.deswater.com

doi: 10.1080/19443994.2015.1072063

57 (2016) 17104–17117
August

Taylor & Francis
Taylor & Francis Group

Equilibrium, kinetic and thermodynamic studies of methyl orange removal by adsorption onto granular activated carbon

G. León*, F. García, B. Miguel, J. Bayo

Departamento de Ingeniería Química y Ambiental, Universidad Politécnica de Cartagena, Paseo Alfonso XIII n° 52, Cartagena 30203, Spain, emails: gerardo.leon@upct.es (G. León), efegeme87@gmail.com (F. García), beatriz.miguel@upct.es (B. Miguel), javier.bayo@upct.es (J. Bayo)

Received 12 March 2015; Accepted 7 July 2015

ABSTRACT

The adsorption of methyl orange (MO) onto granular-activated carbon (AC) is studied. The effects of initial dye concentration, AC dose, initial solution pH, stirring rate, and temperature on MO adsorption were investigated in a batch system. The experimental data were analyzed using the Langmuir, Freundlich, Elovich, Temkin, and Dubinin–Radushkevich adsorption isotherms, and the characteristic parameters and related correlation coefficients were determined for each isotherm at different temperatures. The best fit was achieved by the Langmuir isotherm equation, by increasing the maximum monolayer adsorption capacity from 20.7 to 46.1 mg/g, when the temperature increases from 283 to 313 K. Pseudo-first-order, pseudo-second-order, Elovich, Weber–Morris intraparticle diffusion and Boyd models were used to analyze the kinetic data obtained at different initial MO concentrations. The adsorption kinetic data were well described by the pseudo-second-order model, while the adsorption process was controlled by film diffusion. The Gibbs free energy, enthalpy, and entropy of the adsorption process were also evaluated, the results showing that the adsorption was spontaneous and endothermic under the examined conditions, and was presumably of a physical nature and non-reversible.

Keywords: Methyl orange; Granular-activated carbon; Equilibrium; Kinetic; Thermodynamic

1. Introduction

The removal of hazardous compounds from industrial effluents is one of the greatest environmental challenges faced in recent decades. A considerable amount of colored wastewater is generated from many industries [1]. Dyes usually have a synthetic origin with complex aromatic chemical structures containing different types of organic functional groups, some of them acting as chromophores. More than 100,000 commercial dyes are known and annual production exceeds 70,000 tonnes [2]. Only in the textile industry, the total dye consumption worldwide is more than 10,000 tonnes/year of which, approximately 100 tonnes/year are discharged into water courses [3].

Azo-dyes, characterized by one or more azo-linkages (–N=N–), are the main chemical class of dyes

*Corresponding author.

Presented at the 7th International Conference on Water Resources in the Mediterranean Basin (WATMED7) 8–11 October 2014, Marrakesh, Morocco

used in the industrial field. Methyl orange (MO), widely used in textile, paper, leather tanning, food processing, plastics, cosmetics, rubber, printing, dye manufacturing industries, pharmaceutical industries, and research laboratories, is one of such dyes [4].

The presence of aromatic rings makes the dyes carcinogenic and mutagenic, exerting potent, acute, and/or chronic effects on exposed organisms. They are inert and non-biodegradable when discharged into water courses and they also impart an undesirable color to the same [5], reducing the penetration of sunlight and thereby inhibiting photosynthesis [6]. Toxic amines, produced by the reductive cleavage of azo linkages in the dye molecules, are also released into the environment [7]. These can have a severe effect on humans by damaging the liver, kidneys, brain, central nervous system, and reproductive system [8].

Various techniques have been applied for the removal of azo-dyes from aqueous solutions, including extraction [9], coagulation and flocculation [10], adsorption [11,12], biosorption [12], coprecipitation [13], sonochemical [14] and electrochemical [15] degradations, membrane processes (micellar enhanced ultrafiltration [16], nanofiltration [17], and ion exchange [18]), advanced oxidation processes (Fenton [19] and UV/H_2O_2 photodegradation [20]), and integrated treatments [21].

Among these methods, adsorption is gaining popularity as an effective dye-removal process due to its low initial cost, simplicity of design, ease of operation, insensitivity to toxic substances, high removal efficiency (even in the case of dilute solutions), and the non-formation of harmful substances [22]. It is a useful and simple technique that allows kinetic and equilibrium measurements without the need for highly sophisticated instrumentation [23]. Various potential adsorbents have been assayed for the removal of specific dyes from water.

Among the sorbent materials used, activated carbon (AC) is the most popular for the removal of pollutants from wastewater due to its large porous surface area, controllable pore structure, thermostability, wide spectrum of surface functional groups [24], high adsorption capacity, fast adsorption kinetics, and ease of regeneration [25]. The chemical structure on the carbon surface influences the interaction between polar and non-polar adsorbates. Indeed, the AC adsorption process is recognized as the most promising treatment technology. It involves surface phenomenon by means of which a multicomponent fluid mixture is attracted to the surface of the solid adsorbent, where it forms attachments via physical or chemical interactions [26]. The method is particularly suited to the removal of a large variety of dyes from wastewaters as an alternative to other treatment options [24].

In this paper, we study the removal of MO from aqueous solutions through adsorption onto the commercially available granular AC and analyze the effect of different parameters such as AC dose, initial pH of the MO solution, stirring speed, and temperature. The adsorption process is analyzed through different isotherm and kinetic models, exploring the possible adsorption mechanism and calculating the thermodynamic parameters associated with the adsorption process. No previous studies of the use of this commercial granular AC in the removal of MO have been described.

2. Theoretical

2.1. Equilibrium of adsorption

The adsorption equilibrium, i.e. the equilibrium established between the phase adsorbed on the adsorbent and that in the solution, provides information about the capacity of the adsorbent and it is represented by adsorption isotherms. An adsorption isotherm indicates how the adsorbed molecules are distributed between the liquid and solid phases until the adsorption process reaches a state of equilibrium. This is important for both describing how solutes interact with adsorbents and for optimizing the use of the adsorbent [27].

2.1.1. Langmuir isotherm model

The Langmuir isotherm model assumes a monolayer adsorption, onto an adsorbent surface containing a finite number of adsorption sites, which are equivalent, with no lateral interaction between the adsorbed molecules and no transmigration of adsorbate in the same surface plane. The linearized form of the Langmuir isotherm can be written as [28]:

$$\frac{C_e}{q_e} = \frac{C_e}{q_m} + \frac{1}{q_m K_L} \quad (1)$$

where C_e is the dye concentration in the solution at equilibrium (mg/L), q_e is the dye concentration on the adsorbent at equilibrium (mg/g), q_m is the maximum monolayer adsorption capacity of the adsorbent (mg/g), and K_L is the Langmuir sorption constant (L/ mg). The plot of C_e/q_e vs. C_e should give a straight line with a slope of $1/q_m$ and an intercept of $1/q_m K_L$.

To confirm the favourability of the process, the dimensionless equilibrium parameter R_L was used:

$$R_L = \frac{1}{1 + K_L C_0} \quad (2)$$

where C_0 is the highest initial dye concentration in solution. The R_L value indicates that the adsorption process is favorable ($0 < R_L < 1$), unfavorable ($R_L > 1$), linear ($R_L = 1$), or irreversible ($R_L = 0$) [29].

2.1.2. Freundlich isotherm model

The Freundlich isotherm model assumes heterogeneous surface energies, in which the energy term varies as a function of the surface coverage. The linearized form of the Freundlich model is represented by [30]:

$$\ln q_e = \frac{1}{n} \ln C_e + \ln K_F \quad (3)$$

where K_F and n are constants incorporating the factors affecting adsorption capacity and degree of non-linearity between the solute concentration in the solution and the amount adsorbed at equilibrium, respectively. From the linear plot of $\ln q_e$ vs. $\ln C_e$, the K_F and n values can be determined. The constant K_F, (mg/g) $(L/mg)^{1/n}$, is an approximate indicator of the adsorption capacity, while $1/n$ is a function of the strength of adsorption in the adsorption process [30]: $1/n = 1$ indicates that the partition between the two phases is independent of the concentration, while $1/n < 1$ indicates normal adsorption and $1/n > 1$ indicates cooperative adsorption [30].

2.1.3. Elovich isotherm model

The Elovich isotherm model assumes that the adsorption sites increase exponentially with adsorption, which implies a multilayer adsorption phenomenon. The linearized form of the Elovich isotherm can be written as [31]:

$$\ln \frac{q_e}{C_e} = \ln(K_E q_{mE}) - \frac{q_e}{q_{mE}} \quad (4)$$

where K_E is the Elovich equilibrium constant (L/mg) and q_{mE} is the Elovich maximum adsorption capacity (mg/g). From the linear plot of $\ln(q_e/C_e)$ vs. q_e, the values of the model parameters can be obtained.

2.1.4. Temkin isotherm model

The Temkin isotherm model assumes that the heat of adsorption of all molecules in the layer decreases linearly rather than logarithmically with the coverage and that adsorption is characterized by a uniform distribution of the binding energies, until reaching the maximum binding energy [32]. The model contains a factor that considers the effect of the adsorbate interaction on the adsorbent.

The linearized form of the Temkin model is represented by [32]:

$$\frac{q_e}{q_m} = \frac{RT}{\Delta H} \ln(A C_e) \quad (5)$$

This equation can be written as,

$$q_e = B \ln A + B \ln C_e \quad (6)$$

where B is the Temkin constant related to heat of adsorption ($B = q_m RT/\Delta H$, mg/g), A (L/mg) is the equilibrium binding constant, R is the gas constant (J/mol K), T is the absolute temperature (K), and ΔH is the adsoption energy (J/mol). A plot of q_e vs. $\ln C_e$ should give a linear graph, with B as the slope and B ($\ln A$) as the intercept.

2.1.5. Dubinin–Radushkevich isotherm model (D–R model)

The Dubinin–Radushkevich model, which assumes a heterogeneous surface with a variable sorption potential, is usually used to estimate the apparent free energy of adsorption and to differentiate the physical and chemical adsorption processes.

The linearized form of the Dubinin–Radushkevich model is represented by [33]:

$$\ln q_e = \ln q_m - K\varepsilon^2 \quad (7)$$

where q_m (mg/g) is the theoretical saturation capacity, K is the activity coefficient, related to mean sorption energy (mol^2/J^2), and ε (J/mol) is the Polanyi potential, which is related to the equilibrium concentration as follows:

$$\varepsilon = RT \ln\left(1 + \frac{1}{C_e}\right) \quad (8)$$

The values of the isotherm constants (q_m and K) can be obtained by plotting $\ln(q_e)$ vs. ε^2. The constant K gives the mean free energy of adsorption per molecule of the adsorbate (E (J/mol)) when it is transferred to the surface of the solid from an infinite distance in the

solution. It can be computed using the relationship $E = (2K)^{-1/2}$. The magnitude of E is used to determine the type of adsorption mechanism. An E value of less than 8 kJ/mol indicates physical adsorption, an E value of between 8 and 16 kJ/mol indicates that the adsorption process follows ion-exchange, while an E value of 20–40 kJ/mol indicates chemisorption [34].

The model was used to estimate the apparent free energy of adsorption as well as to differentiate between physical and chemical adsorption process.

2.2. Kinetic of adsorption

Being able to predict the adsorption rate provides important information for choosing and designing the best operating conditions for the full-scale batch process. Adsorption kinetics provides valuable information about the reaction pathways, the mechanism of the reactions, and the mechanisms controlling the adsorption processes, such as mass transfer.

A number of kinetic models have been developed to describe the removal kinetics of dyes and other pollutants, including the pseudo-first-order kinetic model of Lagergren, the pseudo-second-order kinetic model of Ho, and the Elovich kinetic model. To identify the diffusion mechanisms and the rate controlling steps that affect the adsorption process, the Weber and Morris intra-particle diffusion model and the Boyd model can be used.

2.2.1. Pseudo-first-order kinetic model

The Lagergren pseudo-first-order model is based on the assumption that the adsorption rate is proportional to the number of available adsorption sites [35], and is expressed as follows:

$$\frac{dq_t}{dt} = k_{ps1}(q_e - q_t) \tag{9}$$

where k_{ps1} (1/min) is the rate constant of pseudo-first-order adsorption, q_e and q_t (mg/g) are the amounts of the adsorbate adsorbed per gram of adsorbent at equilibrium and at any time t, respectively.

By applying the boundary conditions $t = 0$ to $t = t$ and $q_t = 0$ to $q_t = q_t$, and integrating, the following equation is obtained:

$$\ln(q_e - q_t) = \ln q_e - k_{ps1}t \tag{10}$$

The plot of $\ln(q_e - q_t)$ against t allows the kinetic model to be evaluated and the values of q_e and k_{sp1} to be determined from the intercept and slope, respectively.

2.2.2. Pseudo-second-order kinetic model

The pseudo-second-order kinetic model of Ho is based on the assumption that the adsorption rate is proportional to the square of the number of unoccupied adsorption sites [36]. It is represented by the following equation:

$$\frac{dq_t}{dt} = k_{ps2}(q_e - q_t)^2 \tag{11}$$

where k_{ps2} (g/mg min) is the rate constant of pseudo-second-order adsorption. Integrating the above equation from $t = 0$ to $t = t$ and from $q_t = 0$ to $q_t = q_t$, the following equation is obtained:

$$\frac{1}{(q_e - q_t)} = \frac{1}{q_e} + k_{ps2}t \tag{12}$$

The equation is usually expressed as:

$$\frac{t}{q_t} = \frac{1}{k_{ps2}\,q_e^2} + \frac{t}{q_e} \tag{13}$$

where $k_{ps2}\,q_e^2$ can be regarded as the initial adsorption rate as $t \rightarrow 0$.

The plot of t/q_t against t allows evaluation of the kinetic model and the determination of k_{ps2} and q_e from the intercept and slope, respectively.

2.2.3. Elovich model

The Elovich model assumes that the rate of adsorption decreases exponentially with an increase in the amount of adsorbate adsorbed, and is one of the most useful models for describing chemisorption. This model can be expressed by the following equation [33]:

$$\frac{dq_t}{dt} = \alpha e^{\beta q_t} \tag{14}$$

where q_t (mg/g) is the amount of the adsorbate adsorbed per gram of adsorbent at any time t, α (mg/g min) is the initial adsorption rate, and β (g/mg) is a constant related to the covert surface and to the activation energy of the adsorption process.

Assuming that $\alpha\,\beta\,t >> 1$ [37], this equation can be simplified, and after integrated by applying the

boundary conditions of $q_t = 0$ at $t = 0$ and $q_t = q_t$ at $t = t$, a linear form is obtained [33]:

$$q_t = \frac{\ln(\alpha\beta)}{\beta} + \frac{\ln t}{\beta} \tag{15}$$

The plot of q_t against $\ln(t)$ allows to evaluate the kinetic model and to determine the constants of the model from the slope and from the intercept.

2.3. Adsorption mechanism

The above kinetic models are not able to identify the diffusion mechanisms and the rate controlling steps that affect the adsorption process. Any solid–liquid sorption process is usually characterized by external mass transfer (boundary layer diffusion) or intraparticle diffusion, or both. The following three steps describe the adsorption dynamics [38]:

(1) The adsorbate molecules move from the bulk solution to the external surface of the adsorbent (film diffusion).
(2) Adsorbate molecules move through the interior of the adsorbent particles (particle diffusion).
(3) Sorption of the solute on the interior surface of the pores and capillary spaces of adsorbent (sorption).

The third step in the adsorption dynamics is assumed to be very rapid and can be considered negligible. Steps (1) and (2) can be considered to be acting individually or in combination. In the present study, two kinetic models, namely the Weber–Morris and Boyd models, were used to describe the mechanism of MO adsorption on AC.

2.3.1. Weber Morris model

For design purposes, it is necessary to distinguish between the film diffusion and the intraparticle diffusion of adsorbate molecules. Weber and Morris intraparticle diffusion model [39] was used, which is commonly expressed by,

$$q_t = k_{\text{intp}} t^{1/2} + C_{\text{i}} \tag{16}$$

where k_{intp} (mg/g $\text{h}^{1/2}$), the intraparticle diffusion rate constant, is obtained from the slope of the straight line of q_t vs. $t^{1/2}$. C_{i} represents the boundary layer effect, so that the larger the intercept, the greater the contribution of surface sorption to the rate-controlling step. For pure intraparticle diffusion to take place, the plot of q_t vs. $t^{1/2}$ should be linear, passing through the origin, with no intercept; otherwise, some other mechanism besides intraparticle diffusion will also be involved and the intraparticle diffusion will not be the only rate-controlling step [40]. That is, if the plot shows multilinearity, then the adsorption process may be controlled by the combination of film and intraparticle diffusion, with more than one step involved [41].

2.3.2. Boyd model

To identify the actual slowest step in the adsorption process (film diffusion or intraparticle diffusion step), the Boyd kinetic model was used. The equation that described this model can be expressed as [38]:

$$B_t = -0.4977 - \ln\left(1 - \frac{q_t}{q_{\text{e}}}\right) \tag{17}$$

If the plots of B_{s} against time are linear and pass through the origin, then the rate-controlling step in the adsorption process is particle diffusion. Otherwise, an adsorption process controlled by film diffusion is suggested.

2.4 Thermodynamic of adsorption

Thermodynamic parameters allow us to evaluate the orientation and feasibility of a physicochemical adsorptive process. Both energy and entropy should be taken into account in determining whether a given adsorption process will take place spontaneously. Moreover, the values of the thermodynamic parameters are the real indicators for the practical application of an adsorption process. So, in order to investigate the thermodynamic behavior of an adsorption process, the thermodynamic parameters standard free energy (ΔG°), standard enthalpy (ΔH°), and standard entropy (ΔS°) of the adsorption were estimated from the following equations:

$$\Delta G^\circ = -RT \ln K_{\text{e}} \tag{18}$$

$$\ln K_{\text{e}} = -\frac{\Delta G^\circ}{RT} = -\frac{\Delta H^\circ}{RT} + \frac{\Delta S^\circ}{R} \tag{19}$$

where R is the universal gas constant (8.314 J/mol K), K_{e} is the thermodynamic equilibrium constant, and T is the absolute temperature (K). Values of K_{e} may be calculated from the relation $\ln(q_{\text{e}}/C_{\text{e}})$ vs. q_{e} at

different temperatures and extrapolating to zero [42]. The plot of $\ln K_e$ vs. $1/T$ should give a straight line with a slope of $-\Delta H^{\circ}/R$ and an intercept of $-\Delta S^{\circ}/R$.

3. Experimental

3.1. Materials

Darco AC 4–12 (Sigma Aldrich) was used as adsorbent. Before using, it was washed several times with deionized water to eliminate powder carbon, dried in an oven at 105˚C for 24 h to remove the moisture and stored in a dissicator. Properties of this granular AC are included in Table 1.

MO, supplied by Sigma Aldrich, was used as adsorbate. This dye has a chemical formula of $C_{14}H_{14}N_3NaO_3S$, and a molecular weight of 327.34 g/mol. The chemical structure of MO is shown in Fig. 1.

All of the MO solutions were prepared in distilled water. The pH of the solution was adjusted with HCl or NaOH (both from Probus) solutions using a Crison micro 2,000 pH-meter with a combined pH electrode.

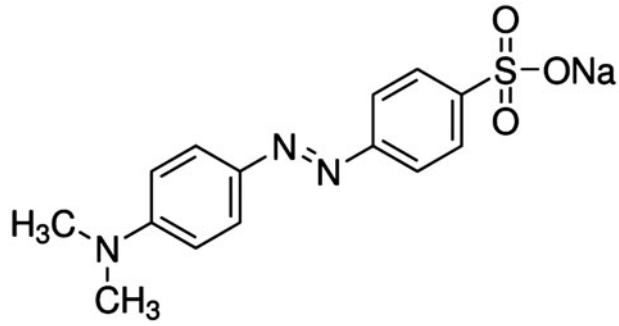

Fig. 1. Chemical structure of MO.

3.2. Methods

3.2.1. Effect of experimental parameters on adsorption process

The effects of initial MO concentration (10–50 mg/L), AC dosage (0.015–0.055 g), initial pH of the dye solution (2.5–10.5), and stirring rate (50–250 rpm) on the adsorption of MO onto commercial AC were studied by varying the parameters under study and keeping other parameters constant. Typical experimental conditions were: initial MO concentration, 20 mg/L; absorbent dose, 20 mg; initial pH of MO solution, 5.7; stirring rate, 200 rpm; and a temperature of 293 K.

Batch experiments were performed in a set of 50 mL Erlenmeyer flasks containing 40 mL of dye solution. The flasks were shaken in a thermostated shaker for 24 h. Samples were taken at different predetermined times and the residual MO concentration in the solution was measured by UV–vis spectrophotometry, at 508 nm, after addition of 1 M HCl, using an Agilent 8453 spectrophotometer.

The percentage of MO removal was obtained by using the following equation:

$$\%\,\text{Removal} = \frac{C_0 - C_e}{C_0} 100 \tag{20}$$

where C_0 and C_e are the initial and equilibrium MO concentrations in the solution (mg/L), respectively.

3.2.2. Equilibrium and kinetic experiments

In the equilibrium and kinetic experiments, the batch adsorption studies were carried out by shaking 0.02 g of AC with 40 mL of different concentrations of MO solution (10–50 mg/) for 24 h at the solution pH (5.7), in a rotary shaker (50 mL Erlenmeyer flasks) at 200 rpm. The temperature was 293 K in the kinetic experiments and 283–313 K in the equilibrium experiments.

The amount of MO loaded onto the AC at any time t, q_t (mg/g), and at equilibrium, q_e (mg/g), was estimated by the following relationships:

Table 1
Properties of commercial AC

Parameter	Value	Parameter	Value
Particle size (mesh)	4–12	Mesopore volume (2–20 μm) (cm^3/g)	0.202[a]
Specific surface area (m^2/g)	520[a]	Total acidity (μeq/g)	212.5[b]
Pore volume (cm^3/g)	0.543[a]	Total basicity (μeq/g)	417.9[b]
Micropore volume (<2 μm) (cm^3/g)	0.219[a]	Cero charge point	4.7[b]
Mesopore volume (2–20 μm) (cm^3/g)	0.122[a]		

[a][43].
[b][44].

$$q_t = (C_0 - C_t)\frac{V}{m} \quad (21)$$

$$q_e = (C_0 - C_e)\frac{V}{m} \quad (22)$$

where C_t is the concentration of MO in the solution at time t (mg/L), V is the volume of MO solution (L), and m is the mass of AC (g).

The data obtained from these experiments were used to test the different isotherm, kinetic, and adsorption mechanism models.

3.2.3. Effect of temperature on adsorption. Thermodynamic study

To study the effect of temperature on the adsorption process, samples of 0.02 g of AC were added to 40 mL of a 50 mg/L MO aqueous solution at the solution pH and the mixtures were shaken in 50 mL stoppered flasks at 200 rpm and different temperatures (283–323 K) for 24 h. Data obtained from these experiments were used to determine the thermodynamic parameters through Eq. (18).

4. Results and discussion

4.1. Effect of experimental parameters

4.1.1. Effect of the initial MO concentration

The initial dye concentration has a pronounced effect on the extent of its removal from aqueous solutions, as shown in Fig. 2(a). The plot shows that increasing the MO concentration from 10 to 50 mg/L decreases the MO removal percentage from 83.78 to 30.58%, and increases the adsorption capacity from 15.43 to 29.71 mg/g. This increase in adsorption capacity with the initial dye concentration may be due to the increase in the driving force to overcome the resistance to the mass transfer of MO between the aqueous phase and the solid phase, enhancing the interaction between MO and AC [45]. The decrease in the percentage of MO removal can be attributed to the saturation of available active sites on the absorbent above a certain concentration of adsorbate [46].

4.1.2. Effect of AC dosage

The quantity of adsorbent used is a very important feature as it determines the extent of dye removal and may be used to determine the cost of adsorbent per unit volume of solution to be treated. The results shown in Fig. 2(b) indicate that the MO removal percentage increases from 24.6 to 94.8% when the AC dosage increases from 0.015 to 0.055 g. This increase can be attributed to an increase in the total available area and, consequently, in the total number of adsorption sites. The MO removal percentage increases sharply when AC dose increases from 0.015 to 0.035 g, but further increase in AC dosage leads to a more moderate increase in MO removal, probably due to the split in the flux or the concentration gradient between the solute concentration in the solution and the solute concentration on the surface of the adsorbent [47].

4.1.3. Effect of the initial pH of the solution

The pH of an aqueous solution is a very influential parameter in the dye adsorption process as it affects the surface charge of the adsorbent material and the degree of ionization of the dye molecule. The effect of initial pH on MO adsorption onto AC is represented in Fig. 2(c), where it can be seen that the MO removal percentage was constant above pH 3 (about 57%) but increased significantly to 79% at lower pH values.

The AC used in this study has a zero charge point of 4.7, and it can be assumed that above this value, active basic groups of the sorbent will be in a neutral form (non-charged), while active acid groups will be ionized (negatively charged). Below pH 4.7, acid groups will be in a neutral form, but basic groups will be protonated (positively charged). In the same way, as MO has a pK_a of 3.5, it can be assumed that above pH 3.5, the dye will have a negative charge (amine group in non-ionized form and sulfonic group in negative charge ionized form), and that below pH 3.5, the dye will have no net charge (amine group in positive charged ionized form and sulfonic group in negative charge ionized form). This means that above pH 4.7, both MO and AC are negatively charged and adsorption by electrostatic interactions is not favoured by any adsorption resulting from Van der Waals interactions between the p electron density of the carbon layers of the AC and the aromatic ring of the dye. At pH values lower than 3.5, AC is positively charged and MO is not charged (though it has a positive and a negative charge in its molecule). In this case, adsorption can result from both Van der Waals interactions and electrostatic interactions between the positive charges of AC and the negative sulfonic groups of MO, thus resulting in an increase of adsorption.

4.1.4. Effect of stirring rate

The effect of stirring rate on MO removal by adsorption on AC is illustrated in Fig. 2(d). As can be

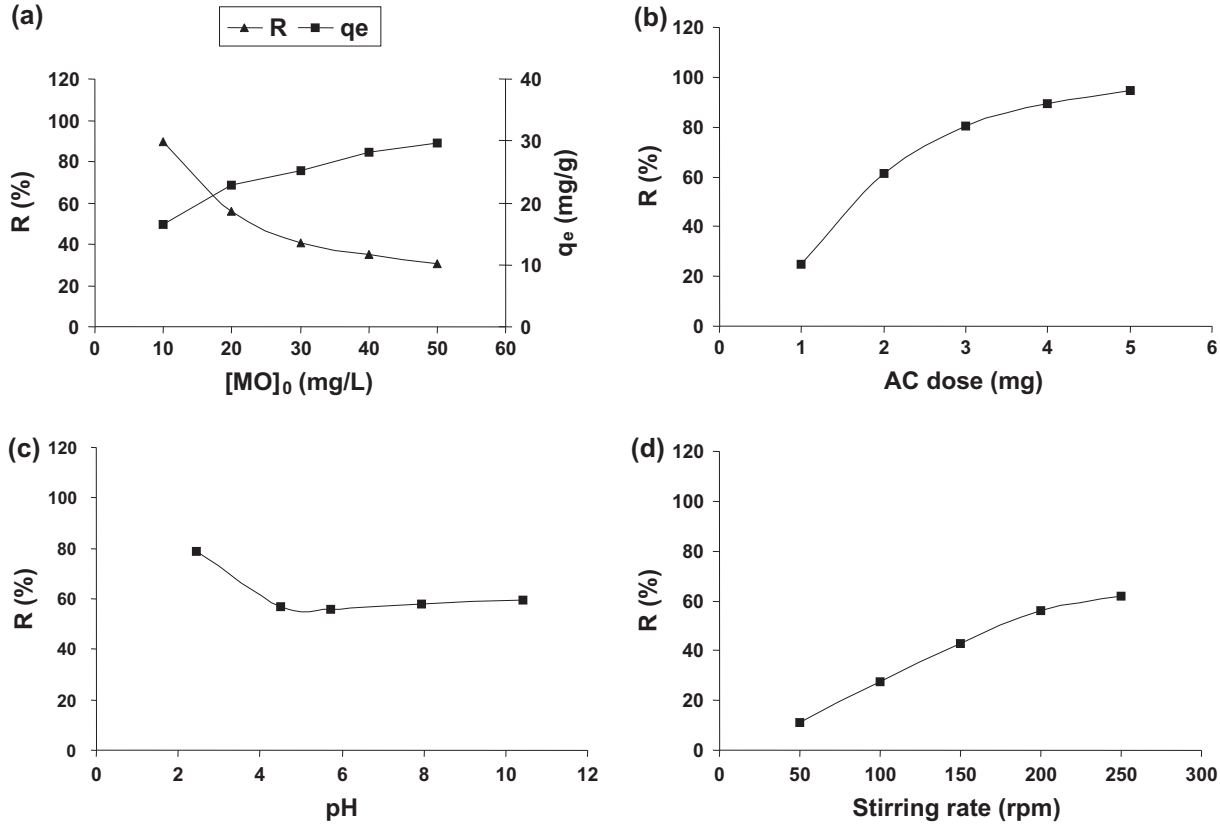

Fig. 2. Effect of different operating variables on MO adsorption onto granular AC: (a) initial MO concentration; (b) AC dose; (c) initial pH of MO solution; and (d) stirring rate.

seen, the MO removal percentage increases with the stirring rate; the increase was greater when the stirring rate increases from 50 to 250 rpm, but lower at higher stirring rate.

So a stirring rate of 200 rpm was selected for further adsorption experiments. This indicates that the diffusion of MO, from the solution into the surface of the adsorbent and into the pores, occurs easily and rapidly.

4.2. Adsorption equilibrium

Linear regression is commonly used to determine the best fitting isotherm to any adsorption process, the applicability of isotherm equations being compared by analyzing the obtained correlation coefficients. So, the experimental equilibrium data of MO adsorption onto AC were analyzed using the Langmuir, Freundlich, Elovich, Temkin, and Dubinin–Radushkevich equations described above.

Linear representation of these models is shown in Fig. 3(a–e), while all the constants and R^2 values obtained from the five isotherm models are included in Table 2.

The Langmuir isotherm model gives the highest R^2 values (0.9796–0.9989). The fit of the experimental data to the Langmuir isotherm model suggests that the surface of AC is made up of homogeneous activated patches. The values of R_L calculated are lower than 1 (0.995–0.998), indicating the favorable character of the MO adsorption process onto AC.

The lower R^2 values obtained for Freundlich, Elovich, Temkin, and Dubinin–Radushkevich equations indicate that these models are not appropriate for describing the adsorption process of MO onto AC.

The free energy value of the adsorption process obtained by the Dubinin–Radushkevich equation (lower than 8 kJ/mol) suggests the physical nature of the adsorption process.

4.3. Adsorption kinetics

The kinetics of MO adsorption onto AC was analyzed by using the Lagergren pseudo-first-order, the

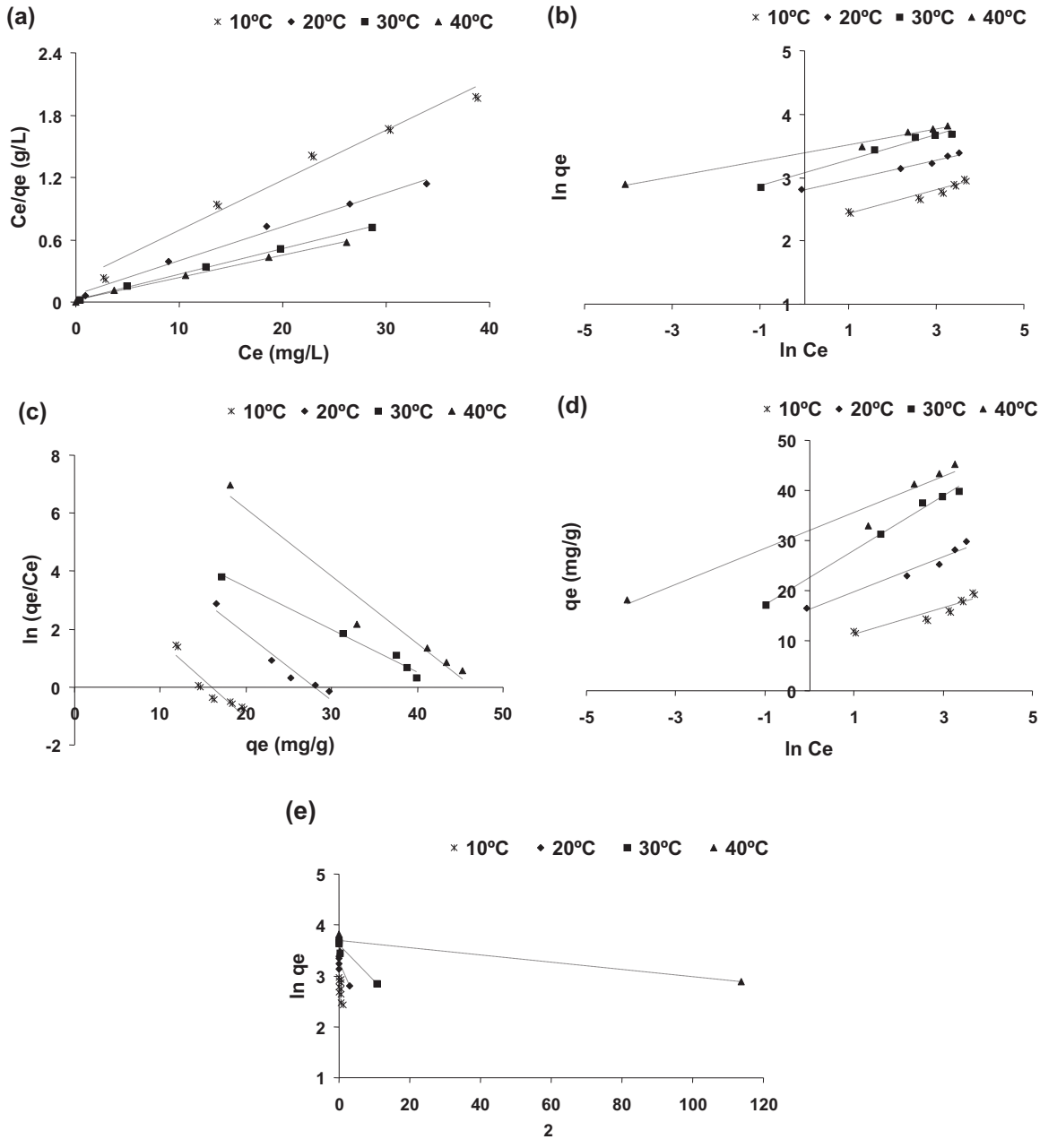

Fig. 3. Isotherm plots for the adsorption of MO onto granular AC: (a) Langmuir; (b) Freundlich; (c) Elovich; (d) Temkin; and (e) Dubinin–Radushkevich.

Ho pseudo-second-order and the Elovich kinetic models described above. Linear representations of these models are shown in Fig. 4(a–c), while all the kinetic parameters and R^2 values calculated from the three kinetic models are included in Table 3.

It is evident from results that the experimental data for MO adsorption onto AC are best described by the pseudo-second-order kinetic model. Table 3 shows that the correlation coefficient R^2 for the pseudo-second-order kinetic equation is greater than 0.99 (0.9915–0.9982) and that the calculated q_e values are in an acceptable agreement with the corresponding experimental values. This confirms that the adsorption data are well represented by the pseudo-second-order kinetic model.

As seen in Table 3, the correlation coefficients of the pseudo-first-order and Elovich kinetic equations are in a range of 0.9538–0.989 and 0.9711–0.9931,

Table 2
Isotherm constants for the adsorption of MO onto granular AC

Temperature (K)	q_m (mg/g)	K_L (L/mg)	R_L	R^2
Langmuir isotherm $\frac{C_e}{q_e}=\frac{C_e}{q_m}+\frac{1}{q_m K_L}$				
283	20.7	0.235	0.998	0.9796
293	30.58	0.45	0.991	0.9901
303	40.98	0.961	0.971	0.9989
313	46.08	1.154	0.955	0.9968
Freundlich isotherm $\ln q_e=\frac{1}{n}\ln C_e+\ln K_F$				
	n	K_F (mg/g) (L/mg)$^{1/n}$		R^2
283	5.49	9.51		0.9392
293	6.28	16.45		0.9871
303	4.96	21.49		0.9809
313	7.99	29.76		0.9906
Elovich isotherm $\ln\frac{q_e}{C_e}=\ln(K_E q_{mE})-\frac{q_e}{q_{mE}}$				
	q_{mE} (mg/g)	K_E (L/mg)		R^2
283	3.79	17.84		0.862
293	4.35	143.29		0.9538
303	6.85	84.27		0.9873
313	4.32	10924.3		0.9569
Temkin isotherm $q_e=B\ln A+B\ln C_e$				
	A (L/mg)	B (mg/g)		R^2
283	22.003	2.7318		0.8986
293	100.96	3.5057		0.9624
303	65.25	5.4202		0.9931
313	6807.32	3.6236		0.9621
Dubinin–Radushkevich isotherm $\ln q_e=\ln q_m-K\varepsilon^2 \quad \varepsilon=RT\ln\left(1+\frac{1}{C_e}\right)$				
	q_m (mg/g)	K (mol^2/J)	E (J/mol)	R^2
283	17.1	0.7040	0.84	0.7016
293	26.47	0.1540	1.80	0.8295
303	36.94	0.0724	2.63	0.9367
313	40.44	0.0079	7.96	0.8965

respectively, meaning that neither of these models is suitable for describing the interaction between MO and AC.

4.4. Adsorption mechanism

The kinetic experimental results were further analyzed by using the Weber and Morris intraparticle diffusion model (Fig. 5(a)). The fact that the plots shown in Fig. 5(a) are not linear over the whole time range, means that more than one step is involved in the adsorption process, and that intraparticle diffusion is not the only rate-limiting mechanism in that adsorption process. That is, the double nature of the intraparticle diffusion plot confirms the presence of both surface adsorption and intraparticle diffusion [48].

To predict the actual slowest step in the adsorption process, the effect of contact time data was tested with the Boyd kinetic plot. From the results shown in Fig. 5(b), it is observed that the plots are linear, but do not pass through the origin, suggesting that the adsorption process is controlled by film diffusion.

4.5. Adsorption thermodynamics

4.5.1. Effect of temperature on adsorption

It is well established that temperature is another factor that greatly influences any adsorption process. Fig. 6(a) shows the effects of temperature on the MO removal percentage at different initial dye concentrations. An increase of temperature from 283 to 313 K

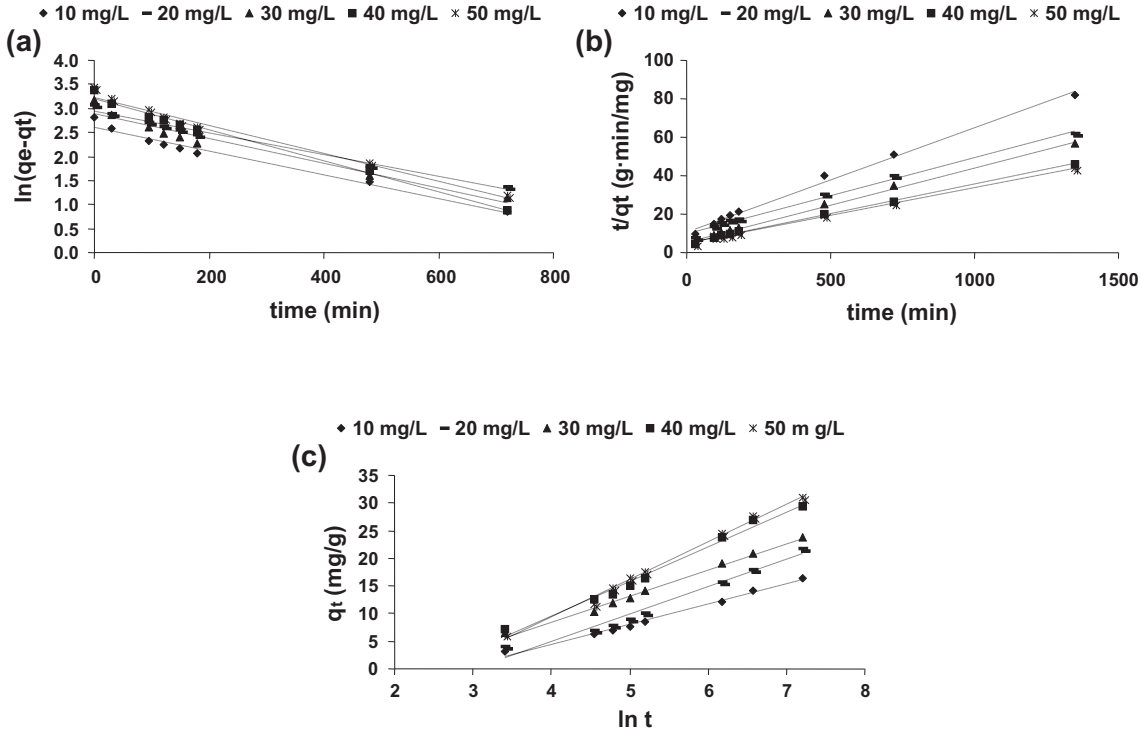

Fig. 4. Kinetic plots for the adsorption of MO onto granular AC: (a) pseudo-first order; (b) pseudo-second order; and (c) Elovich.

Table 3
Kinetic constants for the adsorption of MO onto granular AC

C_0	$q_{e\ (exp)}$	Pseudo-first order			Pseudo-second order			Elovich		
		k_1 (1/min)	$q_{e(calc)}$ (mg/g)	R^2	K_2 (g/mg min)	$q_{e(calc)}$ (mg/g)	R^2	A (mg/g min)	β (g/mg)	R^2
0.10	16.50	0.0025	13.69	0.9764	0.29281685	18.48	0.9945	56.3640	0.2777	0.9905
0.02	22.95	0.0023	18.94	0.9840	0.07842368	25.25	0.9903	98.5992	0.2029	0.9711
0.03	25.24	0.0026	17.99	0.9538	0.04996086	25.83	0.9958	42.8205	0.2117	0.9931
0.04	28.05	0.0032	24.57	0.9890	0.02356701	32.57	0.9972	75.3666	0.1593	0.9853
0.05	29.71	0.0029	25.46	0.9792	0.01682269	34.48	0.9982	92.2357	0.1472	0.9921

leads to an increase of the removal percentage, that is, to an increase in adsorption uptake, for all initial concentrations. This may be due to both an increase in the dye mobility to penetrate inside the adsorbent pores, because of the decrease in solution viscosity, and an increase in the interactions between the dye and functional groups of the AC [49]. These results also suggest that the adsorption of MO onto AC is an endothermic process. It can be also seen from the figure that the percentage removal increases sharply with the increase in temperature up to 303 K, above which the removal percentage reaches an almost constant value.

4.5.2. Thermodynamic parameters

Three thermodynamic parameters were considered in characterizing the adsorption process: the standard free energy (ΔG°), the standard enthalpy (ΔH°), and the standard entropy (ΔS°). ΔG° was calculated from Eq. (18), while ΔH° and ΔS° were calculated from Eq. (19) through the plot of $\ln K_e$ vs. $1/T$ (Fig. 6(b)).

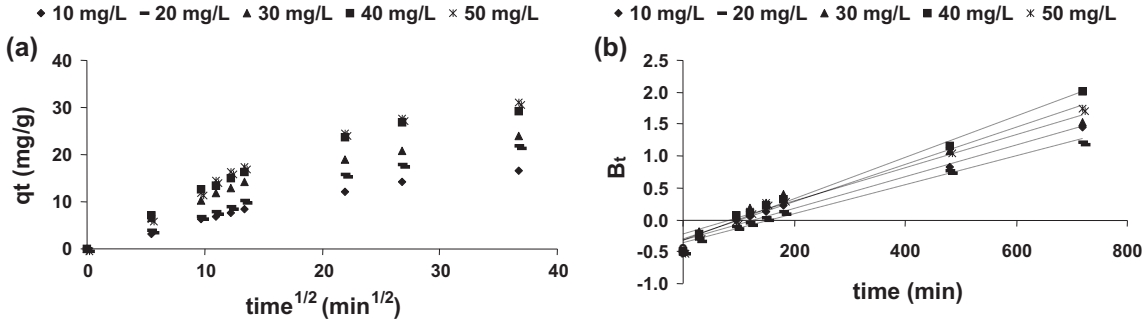

Fig. 5. Adsorption mechanism plots for the adsorption of MO onto granular AC: (a) intraparticle model and (b) Boyd model.

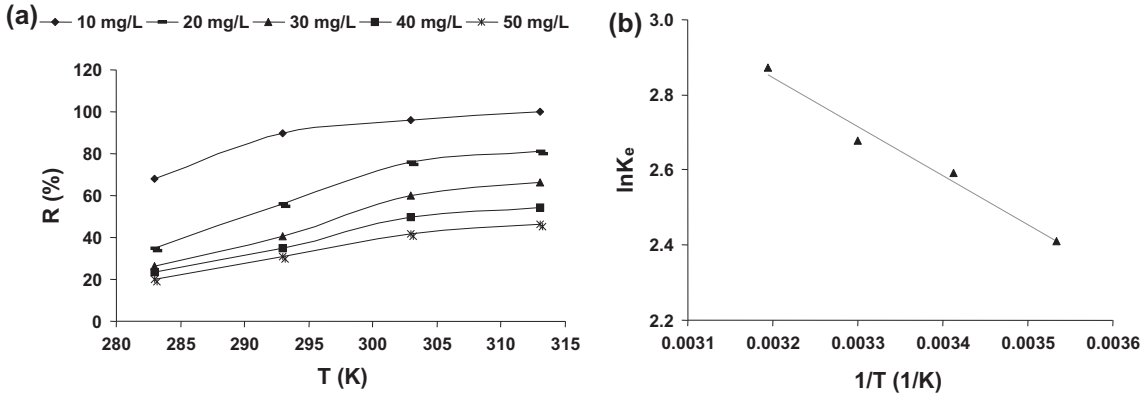

Fig. 6. Thermodynamic of the adsorption of MO onto granular AC: (a) influence of temperature on adsorption and (b) plot of ln K_e vs. $1/T$ for estimating the thermodynamic parameters.

The calculated values of these thermodynamic parameters are shown in Table 4.

As can be seen from Table 4, ΔH° and ΔS° are positive and ΔG° is negative. The adsorption process is obviously spontaneous and thermodynamically favorable with the negative value of ΔG° for all the studied temperatures. Positive values of standard enthalpy (ΔH°) confirm that the adsorption process is endothermic, with adsorption increasing with an increase in temperature. It has been reported that the ΔH° ranges of physiadsorption, ionic exchange, and chemiadsorption are 0–20 kJ/mol, 20–80 kJ/mol, and 80–450 kJ/mol, respectively [50]. In this study, the low value of ΔH° (10.892 kJ/mol) confirms the existence of physiadsorption between MO and AC (electrostatic and Van der Waals interactions). The positive ΔS° value theoretically confirms the affinity of AC for MO adsorption [51] and the non-reversible nature of the adsorption process [52], and suggests the increase of randomness of MO molecules on the AC surface, probably due to structural changes in both the adsorbate and the adsorbent.

Table 4
Thermodynamic parameters of the adsorption of MO onto granular AC

ΔH° (kJ/mol)	ΔS° (kJ/mol K)	ΔG° (kJ)			
		283 K	293 K	303 K	313 K
10.892	0.058	−5.552	−6.133	−6.714	−7.295

5. Conclusion

The adsorption of MO onto granular AC is studied in this paper. The MO removal percentage increases with the carbon dose used, the stirring rate, the temperature and as the pH falls below pH 3 (remaining practically constant at higher pH values), and decreases with the increase in initial dye concentration. Equilibrium data fit the Langmuir isotherm equation very well, and the maximum monolayer adsorption capacity is found to increase from 20.7 to 46.1 mg/g when the temperature increases from 283 to 313 K. The pseudo-second-order kinetic model fits the kinetic data very well. The adsorption mechanism shows that more than one step is involved in the adsorption process and that this is controlled by film diffusion. The negative ΔG° value indicates that the adsorption is feasible and spontaneous. The positive ΔH° and ΔS° values point to the endothermic nature of the adsorption, which presumably has a physical nature. The positive value of ΔS° indicates the affinity of AC for MO adsorption and the non-reversible nature of the adsorption process.

References

[1] S. Wang, J. Wei, S. Lv, Z. Guo, F. Jiang, Removal of organic dyes in environmental water onto magnetic-sulfonic graphene nanocomposite, Clean—Soil Air Water 41 (2013) 992–1001.
[2] T.K. Sen, S. Afroze, H. Ang, Equilibrium, kinetics and mechanism of removal of methylene blue from aqueous solution by adsorption onto pine cone biomass of *Pinus radiata*, Water Air Soil Pollut. 218 (2011) 499–515.
[3] M.T. Yagub, T.K. Sen, H. Ang, Equilibrium, kinetics, and thermodynamics of methylene blue adsorption by pine tree leaves, Water Air Soil Pollut. 223 (2012) 5267–5282.
[4] R. Gong, Y. Ding, M. Li, C. Yang, H. Liu, Y. Sun, Utilization of powdered peanut hull as biosorbent for removal of anionic dyes from aqueous solution, Dyes Pigm. 64 (2005) 187–192.
[5] Z. Aksu, G.A. Dönmez, A comparative study on the biosorption characteristics of some yeasts for Remazol Blue reactive dye, Chemosphere 50 (2003) 1075–1083.
[6] T.O. Mahony, E. Guibal, J.M. Tobin, Reactive dye biosorption by *Rhizopus arrhizus* biomass, Enzyme Microb. Technol. 31 (2002) 456–463.
[7] Z. Aksu, Application of biosorption for the removal of organic pollutants: A review, Process Biochem. 40 (2005) 997–1026.
[8] A.S. Özcan, A. Özcan, Adsorption of acid dyes from aqueous solutions onto acid-activated bentonite, J. Colloid Interface Sci. 276 (2004) 39–46.
[9] A.M. Ferreira, J.A.P. Coutinho, A.M. Fernandes, M.G. Freire, Complete removal of textile dyes from aqueous media using ionic-liquid-based aqueous two-phase systems, Sep. Purif. Technol. 128 (2014) 58–66.
[10] M.A.A. Hassan, P.L. Tan, Z.Z. Noor, Coagulation and flocculation treatment of wastewater in textile industry using chitosan, J. Chem. Nat. Resour. Eng. 4 (2009) 43–53.
[11] J. Wang, H. Ma, W. Yuan, W. He, S. Wang, J. You, Synthesis and characterization of an inorganic/organic modified bentonite and its application in methyl orange water treatment, Desalin. Water Treat. 52 (2014) 7660–7672.
[12] A. Mittal, J. Mittal, A. Malviya, D. Kaur, V.K. Gupta, Decoloration treatment of a hazardous triarylmethane dye, Light Green SF (Yellowish) by waste material adsorbents, J. Colloid Interface Sci. 342 (2010) 518–527.
[13] T. Saitoh, M. Saitoh, C. Hattori, M. Hiraide, Rapid removal of cationic dyes from water by coprecipitation with aluminum hydroxide and sodium dodecyl sulfate, J. Environ. Chem. Eng. 2 (2014) 752–758.
[14] K. Okitsu, K. Iwasaki, Y. Yobiko, H. Bandow, R. Nishimura, Y. Maeda, Sonochemical degradation of azo dyes in aqueous solution: A new heterogeneous kinetics model taking into account the local concentration of OH radicals and azo dyes, Ultrason. Sonochem. 12 (2005) 255–262.
[15] Y. Sun, G. Wang, Q. Dong, B. Qian, Y. Meng, J. Qiu, Electrolysis removal of methyl orange dye from water by electrospun activated carbon fibers modified with carbon nanotubes, Chem. Eng. J. 253 (2014) 73–77.
[16] A.L. Ahmad, S.W. Puasa, M.M.D. Zulkali, Micellar-enhanced ultrafiltration for removal of reactive dyes from an aqueous solution, Desalination 191 (2006) 153–161.
[17] H. Kelewou, A. Lhassani, M. Merzouki, P. Drogui, Removal of textile-based dyes by nanofiltration: Study of physicochemical parameters' effect on the retention by experimental designs methodology, Desalin. Water Treat. 54 (2015) 1735–1746.
[18] J.S. Wu, C.H. Liu, K.H. Chu, S.Y. Suen, Removal of cationic dye methyl violet 2B from water by cation exchange membranes, J. Membr. Sci. 309 (2008) 239–245.
[19] B.H. Hameed, T.W. Lee, Degradation of malachite green in aqueous solution by Fenton process, J. Hazard. Mater. 164(2–3) (2009) 468–472.
[20] M.D. Murcia, M. Gómez, E. Gómez, J.L. Gómez, N. Christofi, Photodegradation of congo red using XeBr, KrCl and Cl_2 barrier discharge excilamps: A kinetics study, Desalination 281 (2011) 364–371.
[21] T.A. Saleh, V.K. Gupta, Photo-catalyzed degradation of hazardous dye methyl orange by use of a composite catalyst consisting of multi-walled carbon nanotubes and titanium dioxide, J. Colloid Interface Sci. 371 (2012) 101–106.
[22] S. Chowdhury, R. Mishra, P. Saha, P. Kushwaha, Adsorption thermodynamics, kinetics and isosteric heat of adsorption of malachite green onto chemically modified rice husk, Desalination 265 (2011) 159–168.
[23] I. Bautista-Toledo, J. Rivera-Utrilla, M.A. Ferro-García, C. Moreno-Castilla, Influence of the oxygen surface complexes of activated carbons on the adsorption of chromium ions from aqueous solutions: Effect of sodium chloride and humic acid, Carbon 32 (1994) 93–100.
[24] G. Mezohegyi, F.P. van der Zee, J. Font, A. Fortuny, A. Fabregat, Towards advanced aqueous dye removal

processes: A short review on the versatile role of activated carbon, J. Environ. Manage. 102 (2012) 148–164.
[25] A.A. Halim, H.A. Aziz, M.A.M. Johari, K.S. Ariffin, Comparison study of ammonia and COD adsorption on zeolite, activated carbon and composite materials in landfill leachate treatment, Desalination 262 (2010) 31–35.
[26] C. Moreno-Castilla, Adsorption of organic molecules from aqueous solutions on carbon materials, Carbon 42 (2004) 83–94.
[27] E. Malkoc, Y. Nuhoglu, Determination of kinetic and equilibrium parameters of the batch adsorption of Cr(VI) onto waste acorn of *Quercus ithaburensis*, Chem. Eng. Process. 46 (2007) 1020–1029.
[28] J. Bayo, G. Esteban, J. Castillo, The use of native and protonated grapefruit biomass (*Citrus paradisi* L.) for cadmium(II) biosorption: Equilibrium and kinetic modelling, Environ. Technol. 33 (2012) 761–772.
[29] J.A. Fernández-López, J.M. Angosto, M.D. Avilés, Biosorption of hexavalent chromium from aqueous medium with opuntia biomass, Sci. World J. (2014) 8 (Article ID 670249), doi: 10.1155/2014/670249.
[30] S. Mohan, J. Karthikeyan, Removal of lignin and tannin colour from aqueous solution by adsorption onto activated charcoal, Environ. Pollut. 97 (1997) 183–187.
[31] S. Chen, J. Zhang, C. Zhang, Q. Yue, Y. Li, C. Li, Equilibrium and kinetic studies of methyl orange and methyl violet adsorption on activated carbon derived from *Phragmites australis*, Desalination 252 (2010) 149–156.
[32] O. Hamdaoui, E. Naffrechoux, Modeling of adsorption isotherms of phenol and chlorophenols onto granular activated carbon Part I. Two-parameter models and equations allowing determination of thermodynamic parameters, J. Hazard. Mater. 147 (2007) 381–394.
[33] Ö. Gök, A. Özcan, B. Erdem, A.S. Özcan, Prediction of the kinetics, equilibrium and thermodynamic parameters of adsorption of copper(II) ions onto 8-hydroxy quinoline immobilized bentonite, Colloids Surf., A: Physicochem. Eng. Aspects 317 (2008) 174–185.
[34] P.S. Kumar, S. Ramalingam, R.V. Abhinaya, S. Dinesh Kirupha, T. Vidhyadevi, S. Sivanesan, Adsorption equilibrium, thermodynamics, kinetics, mechanism and process design of zinc(ii) ions onto cashew nut shell, Can. J. Chem. Eng. 90 (2012) 973–982.
[35] Y. Jiang, H. Pang, B. Liao, Removal of copper(II) ions from aqueous solution by modified bagasse, J. Hazard. Mater. 164 (2009) 1–9.
[36] Y.S. Ho, G. McKay, Pseudo-second order model for sorption processes, Process Biochem. 34 (1999) 451–465.
[37] S.H. Chien, W.R. Clayton, Application of Elovich equation to the kinetics of phosphate release and sorption in soils, Soil Sci. Soc. Am. J. 44 (1980) 265–268.
[38] J. Acharya, J.N. Sahu, B.K. Sahoo, C.R. Mohanty, B.C. Meikap, Removal of chromium(VI) from wastewater by activated carbon developed from Tamarind wood activated with zinc chloride, Chem. Eng. J. 150 (2009) 25–39.
[39] W.J. Weber, J.C. Morris, Kinetics of adsorption on carbon from solution, J. Sanit. Eng. Div. 89 (1963) 31–39.
[40] B.H. Hameed, A.A. Ahmad, N. Aziz, Adsorption of reactive dye on palm-oil industry waste: Equilibrium, kinetic and thermodynamic studies, Desalination 247 (2009) 551–560.
[41] V.C. Srivastava, M.M. Swamy, I.D. Mall, B. Prasad, I.M. Mishra, Adsorptive removal of phenol by bagasse fly ash and activated carbon: Equilibrium, kinetics and thermodynamics, Colloids. Surf., A: Physicochem. Eng. Aspects 272 (2006) 89–104.
[42] N.K. Amin, Removal of direct blue-106 dye from aqueous solution using new activated carbons developed from pomegranate peel: Adsorption equilibrium and kinetics, J. Hazard. Mater. 165 (2009) 52–62.
[43] C.K. Ahn, Y.M. Kim, S.H. Woo, J.M. Park, Selective adsorption of phenanthrene dissolved in surfactant solution using activated carbon, Chemosphere 69 (2007) 1681–1688.
[44] C.K. Ahn, D. Park, S.H. Woo, J.M. Park, Removal of cationic heavy metal from aqueous solution by activated carbon impregnated with anionic surfactants, J. Hazard. Mater. 164 (2009) 1130–1136.
[45] P. Senthil Kumar, K. Ramakrishnan, S. Dinesh Kirupha, S. Sivanesan, Thermodynamic, kinetic, and equilibrium studies on phenol removal by use of cashew nut shell, Can. J. Chem. Eng. 89 (2011) 284–291.
[46] M. Toor, B. Jin, Adsorption characteristics, isotherm, kinetics and diffusion of modified natural bentonite for removing diazo dye, Chem. Eng. J. 187 (2012) 79–88.
[47] P. Senthil Kumar, C. Senthamarai, A. Durgadevi, Adsorption kinetics, mechanism, isotherm, and thermodynamic analysis of copper ions onto the surface modified agricultural waste, Environ. Prog. Sustainable Energy 33 (2014) 28–37.
[48] K.V. Kumar, A. Kumaran, Removal of methylene blue by mango seed kernel powder, Biochem. Eng. J. 27 (2005) 83–93.
[49] A. Tabak, N. Baltas, B. Afsin, M. Emirik, B. Caglar, E. Eren, Adsorption of Reactive Red 120 from aqueous solutions by cetylpyridinium-bentonite, J. Chem. Technol. Biotechnol. 85 (2010) 1199–1207.
[50] T. Calvete, E.C. Lima, N.F. Cardoso, S.L.P. Dias, E.S. Ribeiro, Removal of brilliant green dye from aqueous solutions using home made activated carbons, Clean —Soil Air Water 38 (2010) 521–532.
[51] J. Zhang, D. Cai, G. Zhang, C. Cai, C. Zhang, G. Qiu, K. Zheng, Z. Wu, Adsorption of methylene blue from aqueous solution onto multiporous palygorskite modified by ion beam bombardment: Effect of contact time, temperature, pH and ionic strength, Appl. Clay Sci. 83–84 (2013) 137–143.
[52] J. Deng, Y.S. Shao, N.Y. Gao, S.Q. Zhou, X.H. Hu, Adsorption characteristics of β-ionone in water on granular activated carbon, CLEAN—Soil Air Water 40 (2012) 1341–1348.